Chain dynamics in nonentangled polymer melts: A first-principle approach for the role of intramolecular barriers

5 AUTHORS, INCLUDING:

Marco Bernabei
Universidad Autónoma de Madrid
8 PUBLICATIONS **69** CITATIONS

SEE PROFILE

Emanuela Zaccarelli
Italian National Research Council
109 PUBLICATIONS **4,577** CITATIONS

SEE PROFILE

Francesco Sciortino
Sapienza University of Rome
408 PUBLICATIONS **17,660** CITATIONS

SEE PROFILE

Juan Colmenero
Universidad del País Vasco / Euskal Herriko…
401 PUBLICATIONS **8,519** CITATIONS

SEE PROFILE

PAPER

Chain dynamics in nonentangled polymer melts: A first-principle approach for the role of intramolecular barriers

Marco Bernabei,*[a] Angel J. Moreno,[b] Emanuela Zaccarelli,[c] Francesco Sciortino[c] and Juan Colmenero[abd]

By means of simulations and numerical solutions of the Mode Coupling Theory (MCT), we investigate the role of intramolecular barriers on the chain dynamics of nonentangled polymer melts. We present a global picture by studying the relaxation of the Rouse modes for a wide range of barrier strength, from fully-flexible to stiff chains. Simulations reveal, on increasing the barrier strength, strong deviations from the Rouse model, as anomalous scaling of relaxation times, long-time plateaux, and nonmonotonic wavelength dependence of the mode correlators. These highly non-trivial dynamics are accounted for by the solutions of the MCT equations. We conclude that MCT constitutes a general, first-principle, approach for chain dynamics in nonentangled polymer melts.

I. Introduction

Moderate or strong chain stiffness is present in the majority of polymers and biopolymers. The reason is that most molecular motions in these systems involve jumps in energy over carbon–carbon rotational barriers and/or chain conformational changes. The corresponding map of relaxation processes is largely influenced by the barrier strength, which plays a decisive role in, *e.g.*, crystallization,[1] adsorption in surfaces,[2] and rheological properties.[3]

Accurate predictions of the effects generated by intramolecular barriers constitute a challenge for any microscopic theory of polymer dynamics. A candidate for the latter is the Mode Coupling Theory (MCT) for supercooled liquids.[4–6] By starting from the fundamental Liouville equation of motion and applying the Mori–Zwanzing formalism,[7] generalized Langevin equations are obtained for the time dependence of density correlators. Within the MCT approximations,[4,5] the memory kernel is factorized in terms of the density correlators, leading to a closed set of equations that can be solved numerically. Static correlations enter the memory kernel as external input. These can be supplied from simulation or experiments. However static correlations can also be related, at least formally, to the interaction potential through liquid state theories,[7–9] and in many cases numerically obtained by solving the equations of such

theories. In other words, MCT provides a link between the time dependence of density correlators and the interaction potential. In this sense, MCT constitutes a first-principle theory for slow dynamics in complex systems.

Recently, Chong *et al.* have extended MCT to polymer melts.[10,11] By exploiting the polymer reference interaction site model (PRISM),[8] the MCT equations are considerably simplified. This is achieved by replacing site-specific intermolecular surroundings of a monomer by an averaged one (equivalent site approximation), whereas the full intramolecular dependence is retained in the MCT equations.[10,11] The approach of Chong *et al.*[10,11] was applied to the specific case of fully-flexible chains, *i.e.*, without intramolecular barriers. A major success was the derivation, from first-principles, of the scaling laws predicted by the phenomenological Rouse model[12] for chain dynamics in nonentangled polymer melts.

Despite the extreme simplifications introduced by the Rouse model (see below), its predictions are highly successful for fully-flexible chains.[13] However, the presence of strong intramolecular barriers in many real polymers violates the main assumption of the Rouse model: the gaussian behaviour of static and dynamic intrachain correlations at all length scales. Though gaussian behaviour is recovered at sufficiently large length scales,[14–16] significant non-Rouse effects appear at relevant short and intermediate scales as chains become stiffer.[14–16] This observation suggests the need of a general approach, beyond the fully-flexible limit, for any microscopic theory of nonentangled chain dynamics in real polymers.

In this article we show that this general, first-principle, approach is provided by MCT. We extend our previous study of the role of intramolecular barriers on the glass transition of polymer melts,[17,18] to a broader range of time and length scales probing relaxation of the chain degrees of freedom. By means of simulations and numerical solutions of the MCT equations, we

[a]Donostia International Physics Center, Paseo Manuel de Lardizabal 4, E-20018 San Sebastián, Spain. E-mail: sckbernm@ehu.es
[b]Centro de Física de Materiales (CSIC, UPV/EHU) and Materials Physics Center MPC, Paseo Manuel de Lardizabal 5, E-20018 San Sebastián, Spain
[c]Dipartimento di Fisica and CNR-ISC, Università di Roma La Sapienza, Piazzale Aldo Moro 2, I-00185 Roma, Italy
[d]Departamento de Física de Materiales, Universidad del País Vasco (UPV/EHU), Apartado 1072, E-20080 San Sebastián, Spain

study relaxation of the Rouse modes in a polymer model with intramolecular barriers of tunable strength. We investigate a wide range of barrier strength between the limits of fully-flexible and stiff chains. Simulations reveal highly non-trivial dynamic features for the Rouse modes, as anomalous scaling of relaxation times, long-time plateaus, and nonmonotonic wavelength dependence of the mode correlators. These features are accounted for by the numerical solutions of MCT. Thus we conclude that MCT constitutes a general, first-principle, approach for dynamics in nonentangled polymer melts, for a wide range of barrier strength. The corresponding time and-length scales extend from the caging regime prior to the α-relaxation (as shown in[17,18]), to the relaxation of the slowest Rouse mode (as shown in this article).

II. Methods

We simulate bead-spring chains of $N = 10$ identical monomers of mass m and diameter σ. Monomers at a distance r interact through the potential $V(r) = 4\varepsilon[(\sigma/r)^{12} - 7c^{-12} + 6c^{-14}(r/\sigma)^2]$, which is cut-off at $r/\sigma = c = 1.15$. Connected monomers also interact through a bonding potential[21] $V_{\text{bond}}(r) = -\varepsilon_{\text{bond}}\ln[1 - (r/R_0)^2]$, with $\varepsilon_{\text{bond}}/\varepsilon = 33.75$ and $R_0/\sigma = 1.5$. We implement intramolecular barriers by means of the bending (V_B), and torsion (V_T) potentials proposed by Bulacu and van der Giessen.[19,20] These are defined for each i-momomer ($i \in [1,N]$) as: $V_B(\theta_i) = (\varepsilon K_B/2)(\cos\theta_i - \cos\theta_0)^2$, and $V_T(\theta_i, \theta_{i+1}, \phi_{i,i+1}) = \varepsilon K_T\sin^3\theta_i\sin^3\theta_{i+1}\sum_{n=0}^{3}a_n\cos^n\phi_{i,i+1}$. Chain stiffness is tuned by varying K_B and K_T. θ_i is the bending angle defined by the set ($i - 1, i, i + 1$). $\phi_{i,i+1}$ is the dihedral angle between the planes defined by the sets ($i-1, i, i + 1$) and ($i, i + 1, i + 2$). Following[19,20] we use $\theta_0 = 109.5°$, $a_0 = 3.00$, $a_1 = -5.90$, $a_2 = 2.06$, and $a_3 = 10.95$. Simulations for this simple model of intramolecular barriers reproduce qualitative features observed in real polymers.[19,20] For example, they rationalize non-trivial trends exhibited by the exponents z for the N-dependence of the diffusivity, $D \sim N^{-z}$, below and above the entanglement length, as well as by the temperature dependence of such exponents (see the discussion in Ref. [19,20]).

Temperature T, time t, and length are given respectively in units of ε/k_B (where k_B is the Boltzmann constant), $\sigma(m/\varepsilon)^{1/2}$, and σ. Simulation units can be qualitatively mapped to real units as $\sigma \sim 5$–10 Å, $\sigma(m/\varepsilon)^{1/2} \sim 1$–$10$ ps, and $\varepsilon/k_B \sim 300$–500 K (see the discussion in, e.g., Ref. [21,22]). We simulate a fixed monomer melt density $\rho\sigma^3 = 1$. Additional numerical details can be found in Ref. [17,18].

III. Results

The investigated range of barrier strength corresponds to a strong variation of the chain stiffness. This can be quantified by the characteristic ratio $C_N = \langle R_{\text{ee}}^2\rangle/(N\langle b^2\rangle)$ (in this case $N = 10$), where R_{ee} and b denote respectively the chain end-to-end radius and the bond length. Brackets denote ensemble average. Fig. 1 displays the obtained values of C_{10} at all the investigated state points (K_B, K_T, T). As expected, chain stiffness is enhanced by increasing the strength of the barriers and by decreasing temperature. Moreover, the effect of temperature is much more pronounced in chains with strong barriers than in fully-flexible
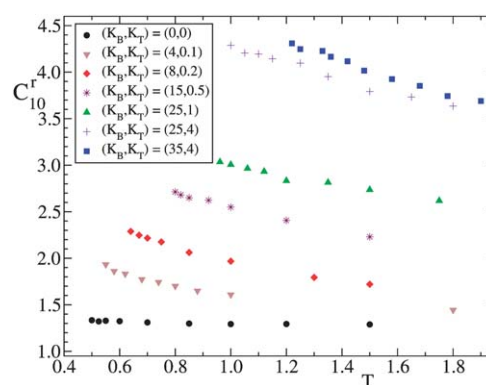

Fig. 1 Temperature dependence of the characteristic ratio C_{10} for all the investigated state points.

chains, for which C_{10} is nearly T-independent. The investigated state points cover a broad range of stiffness, with values of C_{10} varying from $C_{10} \approx 1.3$ for fully-flexible chains up to $C_{10} = 4.3$ for the strongest barriers, (K_B, K_T) = (35, 4), at the lowest investigated T.[23,24]

In the Rouse model[12,25] a tagged chain is represented as a string of N beads (with position vectors $\mathbf{r}_j$) connected by harmonic springs of constant $3k_BT/b^2$. The effective interaction of the tagged chain with its surroundings is given by a friction coefficient ζ and a set of δ-correlated external random forces $\mathbf{f}_j$, $\langle \mathbf{f}_j(t)\cdot\mathbf{f}_k(t')\rangle = 6\zeta k_BT\delta_{jk}\delta(t - t')$. The chain motion is mapped onto a set of N normal modes (Rouse modes) labelled by $p = 0,1,2,\ldots,N - 1$, of wavelength N/p, and defined as $X_p(t) = \sum_{j=1}^{N}P_{jp}\mathbf{r}_j(t)$, with $P_{jp} = \sqrt{(2 - \delta_{p0})/N}\cos[(j - 1/2)p\pi/N]$. $\mathbf{X}_0(t)/\sqrt{N}$ coincides with the chain center-of-mass position. The mode correlators, the central quantities of the present investigation, are defined as $C_{pq}(t) = [\langle X_p(0)\cdot X_q(t)\rangle - \delta_{0,p\times q}\langle X_p(0)\cdot X_q(0)\rangle]/3N$. Furthermore we define the quantities $\hat{C}_{pq}(0) = C_{pq}(0)$ for $p,q > 0$. The properties of the random forces in the Rouse model lead to orthogonality and exponentiality of the Rouse modes,[12] i.e., $C_{pq}(t) = \hat{C}_{pq}(0)\exp[-t/\tau_p]$, with $\hat{C}_{pq}(0) = \delta_{pq}(b^2/24N^2)\sin^{-2}[p\pi/2N]$ and $\tau_p = (\zeta b^2/12k_BT)\sin^{-2}[p\pi/2N]$. Thus, according to the Rouse model, for $p \ll N$, $\hat{C}_{pp}(0)$ and τ_p scale as $\sim p^{-2}$.

In Fig. 2 we show the effect of the barrier strength on intra-chain static correlations. We compute the terms $\Psi_{pq} = \langle X_p(0)\cdot X_q(0)/(X_p(0)X_q(0))\rangle$, where $X_p(0)$ is the modulus of the vector $X_p(0)$. By construction $\Psi_{pq} \equiv 1$ for $p = q$. Data for fully-flexible chains (not shown) exhibit small deviations from orthogonality, indeed $|\Psi_{pq}| < 0.05$ for all $p \neq q$, independently of T. Instead, orthogonality is clearly violated for strong intra-molecular barriers, as shown in the contour plot of Fig. 2a. Moreover, deviations are enhanced by decreasing T. Having noted this, modes p,q of distinct parity fulfil $|\Psi_{pq}| < 0.1$, i.e., they are approximately orthogonal even for the stiffest investigated system. Fig. 2b shows the diagonal terms $\hat{C}_{pp}(0)$ normalized by $\hat{C}_{11}(0)$. Data for fully-flexible chains approximately follow gaussian behaviour, $\hat{C}_{pp}(0) \sim p^{-2.2}$.[13] The introduction of chain stiffness leads to strong non-gaussian behaviour, which can be quantified at intermediate and low p by an approximate power law $\hat{C}_{pp}(0) \sim p^{-x}$, with higher x-values for stronger barriers.[15,26]
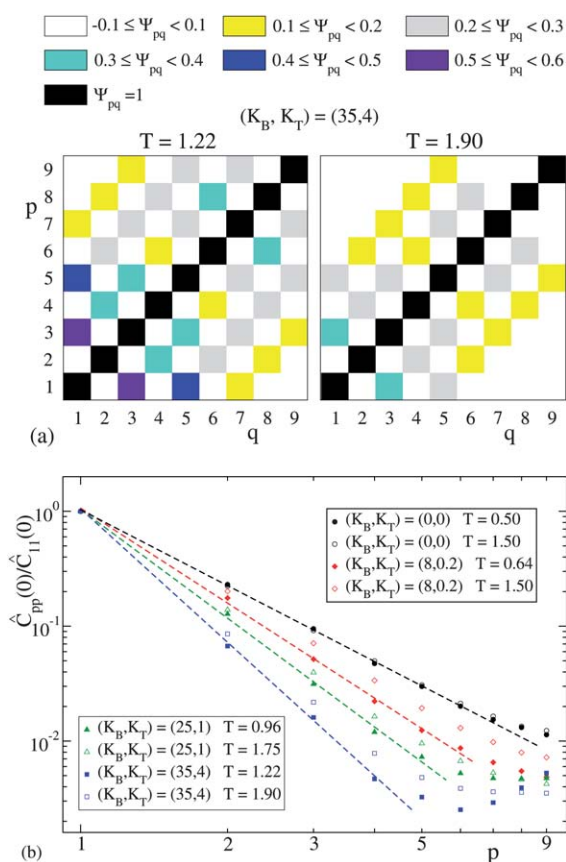
Fig. 2 Static intrachain correlations computed from simulations. For each value of (K_B, K_T) (see legends) results include data at the highest and lowest investigated T. (a): For stiff chains with $(K_B, K_T) = (35, 4)$, contour plot of Ψ_{pq} (see text). (b): Diagonal terms $\hat{C}_{pp}(0)$ (see text) normalized by $\hat{C}_{11}(0)$ for the sake of clarity. Each data set corresponds to a fixed value of (K_B, K_T) and T (see legend). Dashed lines indicate approximate power-law behaviour $\sim p^{-x}$. From top to bottom, $x = 2.2$, 2.7, 3.1, and 3.8.

In the case $(K_B, K_T) = (35, 4)$, at the lowest investigated T, we find $x = 3.8$. The most local effects of intramolecular barriers are manifested by flattening of $\hat{C}_{pp}(0)$ at large p. The non-gaussian behaviour in the systems with intramolecular barriers is observed for all p-values, *i.e.*, it persists over all the length scale of the chain. For the same barrier strength, gaussian statistics will be recovered at values of the mode wavelength, N/p, that can only be probed by chains longer than those ($N = 10$) investigated here. See, *e.g.*, Ref. [15,16] for a realization, in longer chains, of this crossover from anomalous to Gaussian scaling in $\hat{C}_{pp}(0)$.

The introduction of chain stiffness also has dramatic effects in the dynamics. Fig. 3 shows results for the relaxation time τ_1 of the mode $p = 1$ *versus* the characteristic ratio of the investigated systems at fixed $T = 1.5$. Relaxation times τ_p for the different p-modes are operationally defined as $\Phi_{pp}(\tau_p) = 0.3$, where $\Phi_{pp}(t) = C_{pp}(t)/\hat{C}_{pp}(0)$ is the normalized Rouse correlator. The obtained time τ_1 at $T = 1.5$ increases by about two decades over the investigated range of stiffness.

Fig. 4 displays, for several values of (K_B, K_T) and T, the p-dependence of the times τ_p. The latter show analogous trends to those observed in Fig. 2 for the static amplitudes $\hat{C}_{pp}(0)$. Fully-flexible chains exhibit approximate Rouse scaling $\tau_p \sim p^{-2}$.
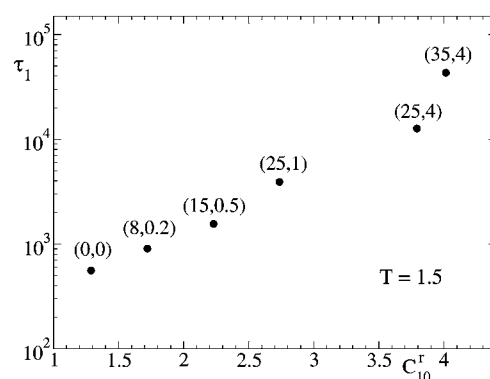

Fig. 3 Relaxation time τ_1 of the mode $p = 1$ *versus* the characteristic ratio C_{10}^r at fixed temperature $T = 1.5$. The respective values of (K_B, K_T) are indicated on top of each symbol.

Strong deviations are instead observed as chains become stiffer. We again quantify the latter by effective power-laws $\tau_p \sim p^{-x}$. As observed for $\hat{C}_{pp}(0)$, x is weakly dependent on T[27] but strongly dependent on the barrier strength, taking higher values for stiffer chains. The x-values for $\hat{C}_{pp}(0)$ and τ_p at the same (K_B, K_T) and T are similar, indicating that the structural origin of the observed dynamic anomalies is mainly controlled by intrachain static correlations.

Fig. 5a displays simulation results of the normalized mode correlators $\Phi_{pp}(t)$, for $(K_B, K_T) = (35, 4)$, at $T = 1.48$. Several salient features are revealed. First, the unambiguous presence of a long-time plateau for the modes $p = 3$ and $p = 5$, followed by an ultimate slow decay. Note that this is not related to the structural α-relaxation associated to the proximity of the glass transition. Indeed it arises at times far beyond the α-time scale ($\sim 5 \times 10^{-3} \tau_1$ at this T). This feature is instead intimately connected to the relaxation of the internal torsional degrees of freedom of the chain. Indeed we observe (not shown) that for fixed bending constant K_B, the long-time plateau tends to vanish as the value of the torsional constant K_T is decreased.
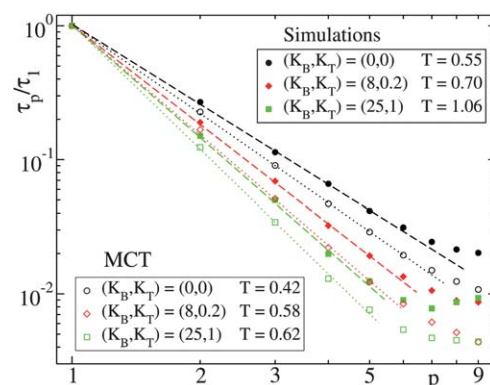

Fig. 4 The p-dependence of the relaxation times τ_p of the mode correlators. Filled symbols: simulations. Empty symbols: MCT numerical solutions. Each data set corresponds to a fixed value of (K_B, K_T) and T (see legends). For clarity, each set is rescaled by its respective τ_1. Dashed and dotted lines indicate approximate power-law behaviour $\sim p^{-x}$. From top to bottom, simulations (dashed): $x = 2.0$, 2.4, 2.8; MCT (dotted): $x = 2.2$, 2.7, 3.1.
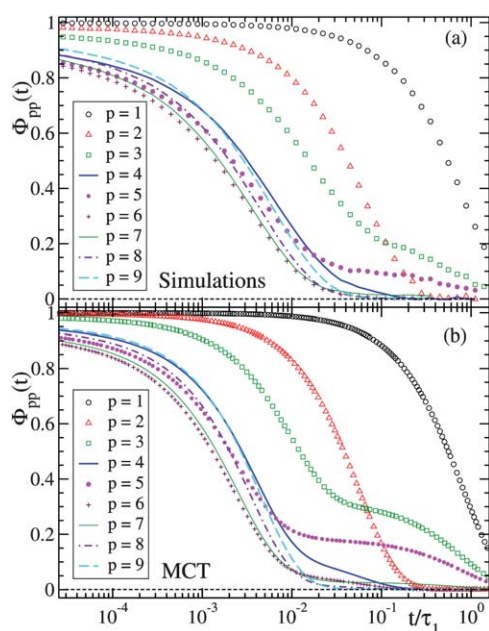
Fig. 5 Normalized mode correlators $\Phi_{pp}(t)$ for stiff chains with $(K_B, K_T) = (35, 4)$. Panel (a): simulation results at $T = 1.48$. Panel (b): MCT numerical solutions at $T = 0.63$. In both panels, the absolute time is rescaled by the relaxation time τ_1 of the mode $p = 1$.

The long-time plateau constitutes a clear breakdown of the Rouse model, which predicts single, purely exponential decays of the mode correlators. Its origin can be tentatively understood as follows. Relaxation of the pth-mode is equivalent to relaxation of a harmonic oscillation of wavelength N/p. For strong torsional barriers, the wavelengths of some particular modes probe characteristic lengths over which chain deformation involves a strong energetic penalty (due to the presence of the barriers). Thus, at the time scales for which the barrier amplitudes are probed, relaxation of such modes becomes strongly hindered, leading to the observed long-time plateau regime and ultimate slow relaxation. Another intriguing feature of Fig. 5a, also inconsistent with the Rouse model predictions, is the nonmonotonic p-dependence of the mode correlators at intermediate times prior to the long-time plateau (see data for $p > 4$).

IV. Discussion

All these highly non-trivial dynamic features can be rationalized in terms of the PRISM-based MCT approach of Chong *et al.* Note that the PRISM approximations retain their validity not only in the fully-flexible limit,[28] but also when strong intramolecular barriers are present.[18] We solved the MCT equations for the mode correlators,[11]

$$\ddot{C}_{pq}(t) + \frac{k_B T}{mN}\delta_{0p}\delta_{0q} + \frac{k_B T}{m}\sum_{s=0}^{N-1} E_{ps} C_{sq}(t)$$
$$+ \frac{k_B T}{m}\sum_{s=0}^{N-1}\int_0^t dt' m_{ps}(t-t')\dot{C}_{sq}(t') = 0, \quad (1)$$

which are derived from the respective MCT equations for the self site-site density correlators in the limit of wave vector $k \rightarrow 0$ (see Ref. [11]). In eqn (1) $E_{pq} = (1 - \delta_{0,p\times q})\hat{C}_{pq}^{-1}(0)/N$, with

$\hat{C}_{pq}^{-1}(0)$ the inverse matrix of $\hat{C}_{pq}(0)$. The memory kernel reads $m_{pq}(t) = (\rho/6\pi^2)\int dk k^4 S(k)c^2(k)\sum_{i,j=1}^{N} P_{ip} F_{ij}^s(k, t)P_{jq}\phi(k, t)$. The coherent density correlators $\phi(k, t)$ and self site-site density correlators $F_{ij}^s(k, t)$ are calculated by solving the associated MCT equations for the density fluctuations (see Ref. [11]). The static structure factor, $S(k)$, and the direct correlation function, $c(k)$, enter the former equations as external inputs. They were evaluated[18] by combining simulation results of the chain form factor, $\omega(k)$, with the PRISM[8] $\rho c(k) = 1/\omega(k) - 1/S(k)$ and the Percus–Yevick[7] closure relations. The static quantities $\hat{C}_{pq}(0)$ and $\hat{C}_{pq}^{-1}(0)$, which also enter eqn (1) as external inputs, were directly computed from the simulations. MCT equations were numerically integrated as described in Ref. [29].

Fig. 5b shows the MCT solutions for the normalized mode correlators of the stiffest investigated chains at $T = 0.63$. The separation parameter $\varepsilon_T = T/T_c - 1 \lesssim 0.2$ is the same as the simulated $T = 1.48$ [data in Fig. 5a] for the same barrier strength.[30] A full correspondence with the simulation trends is obtained, including the long-time plateaux for $p = 3$ and 5, as well as the sequence in the complex, nonmonotonic p-dependence for $p > 4$ at intermediate times. Fig. 4 shows the p-dependence of the relaxation times τ_p (as defined above) of the mode correlators obtained from solving the MCT equations. These are compared with simulation data for several values of (K_B, K_T), at common $\varepsilon_T \lesssim 0.2$. Again, MCT solutions are in semiquantitative agreement with the anomalous trends of simulations, with similar exponents for the effective power-laws. Thus, changes in the *static* intrachain correlations (induced by increasing stiffness) enter the MCT equations and yield the corresponding changes in the dynamic correlations. Slaving the dynamics to statics is indeed the essence of MCT.[31] It is worth noting that, since mode correlators are well described by MCT, the agreement with simulations is similar for other observables probing chain dynamics as, *e.g.*, the orientational bond correlator (not shown). The reason is that such observables can be formally expressed as combinations of the mode correlators.[12]

5. Conclusions

We have presented a global picture of the chain dynamics of a realistic model for nonentangled polymer melts, which incorporates intramolecular barriers of tunable strength. By increasing the barrier strength between the limits of fully-flexible and stiff chains, strong deviations from the Rouse model are revealed. MCT accounts for the anomalous scaling of the relaxation times, the long-time plateaux, and the nonmonotonic wavelength dependence of the mode correlators. Thus, MCT is established as a first-principle theory for dynamics of nonentangled real polymers, for a wide range of barrier strength. It describes a broad dynamic range, from the caging characteristic time to the relaxation time of the slowest Rouse mode.

Notes and references

1 H. Meyer and F. Müller-Plathe, *Macromolecules*, 2002, **35**, 1241–1252.
2 E. Y. Kramarenko, R. G. Winkler, P. G. Khalatur, A. R. Kokhhlov and P. Reineker, *J. Chem. Phys.*, 1996, **104**, 4806–4813.
3 D. C. Morse, *Macromolecules*, 1998, **31**, 7044–7067.
4 W. Götze, *Rep. Prog. Phys.*, 1992, **55**, 241–376.
5 W. Götze, *Complex Dynamics of Glass-Forming Liquids. A Mode Coupling Theory*, Oxford University Press, New York, 2009.
6 It is well-known that ideal MCT fails in describing the slow structural α-relaxation associated to the glass transition, beyond the moderately supercooled regime. Thus, a unified description of structural relaxation and internal chain dynamics in terms of MCT excludes the case of the *deeply* supercooled regime. The conclusions made in the rest of the article must be understood under this limitation.
7 J.-P. Hansen and I. R. McDonald, *Theory of Simple Liquids*, Academic Press, London, 2006.
8 K. S. Schweizer and J. G. Curro, *Adv. Chem. Phys.*, 1997, **98**, 1–142.
9 M. Pütz, J. G. Curro and G. S. Grest, *J. Chem. Phys.*, 2001, **114**, 2847–2860.
10 S.-H. Chong and M. Fuchs, *Phys. Rev. Lett.*, 2002, **88**, 185702.
11 S.-H. Chong, M. Aichele, H. Meyer, M. Fuchs and J. Baschnagel, *Phys. Rev. E: Stat., Nonlinear, Soft Matter Phys.*, 2007, **76**, 051806.
12 M. Doi and S. F. Edwards, *The Theory of Polymer Dynamics*, Oxford University Press, Oxford, 1986.
13 C. Bennemann, J. Baschnagel, W. Paul and K. Binder, *Comput. Theor. Polym. Sci.*, 1999, **9**, 217–226.
14 W. Paul, G. D. Smith and D. Y. Yoon, *Macromolecules*, 1997, **30**, 7772–7780.
15 S. Krushev, W. Paul and G. D. Smith, *Macromolecules*, 2002, **35**, 4198–4203.
16 M. O. Steinhauser, J. Schneider and A. Blumen, *J. Chem. Phys.*, 2009, **130**, 164902.
17 M. Bernabei, A. J. Moreno and J. Colmenero, *Phys. Rev. Lett.*, 2008, **101**, 255701.
18 M. Bernabei, A. J. Moreno and J. Colmenero, *J. Chem. Phys.*, 2009, **131**, 204502.
19 M. Bulacu and E. van der Giessen, *J. Chem. Phys.*, 2005, **123**, 114901.
20 M. Bulacu and E. van der Giessen, *Phys. Rev. E: Stat., Nonlinear, Soft Matter Phys.*, 2007, **76**, 011807.
21 K. Kremer and G. S. Grest, *J. Chem. Phys.*, 1990, **92**, 5057–5086.
22 J. Baschnagel and F. Varnik, *J. Phys.: Condens. Matter*, 2005, **17**, R851–R953.
23 The data of C_{10}^{r} given here are considerably smaller than the limit C_{∞}^{r} estimated from simulations or experiments on much longer chains. This is clearly a finite size effect. Thus, at $T = 1.0$ we find $C_{10}^{r} = 3.0$ for $(K_B, K_T) = (25,1)$. Data in Ref. [19] for the same model of intramolecular barriers and much longer chains ($N = 200$) provide an estimation of C_{∞}^{r}, with a value almost twice larger, $C_{200}^{r} = 5.8$, than C_{10}^{r} for the former (K_B, K_T, T). The value $C_{\infty}^{r} \geq C_{200}^{r} = 5.8$ is comparable to characteristic ratios of, *e.g.*, polybutadiene and polypropylene.[24] The stiffest case investigated here (not studied in Ref. [19]), will presumably yield values $C_{\infty}^{r} \sim 10$, similar to that of polystyrene[24].
24 M. Rubinstein and R. H. Colby, *Polymer Physics*, Oxford University Press, New York, 2003.
25 We use the normalizations introduced for the MCT equations of Ref. [11] and eqn (1) in this article.
26 The exponent $x \approx 3$ observed for $(K_B, K_T) = (25, 1)$ at $T \approx 1$ (Fig. 2b) is similar to that found in simulations of polybutadiene[15] with chemically realistic force fields. This is consistent with the similar values of C_{∞}^{r} obtained for this polymer and for the bead-spring model at the former state point (see end note [23]).
27 For example, for $(K_B, K_T) = (25, 1)$ we find a variation of $\approx 7\%$ in x for a change in T by a factor ~ 2.
28 M. Aichele, S.-H. Chong, J. Baschnagel and M. Fuchs, *Phys. Rev. E: Stat., Nonlinear, Soft Matter Phys.*, 2004, **69**, 061801.
29 W. Götze, *J. Stat. Phys.*, 1996, **83**, 1183–1197.
30 T_c is the MCT temperature for structural arrest.[4,5] The mean-field character of MCT yields a large drift between simulation ($T_c^{MD} = 1.23$) and theory ($T_c^{MCT} = 0.54$). Moreover, MCT times are affected by an undetermined constant factor.[4,5] Thus, a proper comparison between theory and simulation can be done by rescaling t by some characteristic relaxation time (τ_1 here) and using a common ε_T[11].
31 The kernel of eqn (1) is dominated by contributions around the maximum of $S(k)$ which fully decay at times $t \gg \tau_{\alpha}$ (as the times τ_p of the slowest modes).[11] Phenomenological models based on Markovian approximations, as *e.g.*[32,33] for semiflexible chains or the Rouse model in the fully-flexible limit, may then be invoked. Thus, by using $\delta(t)$-like functions in the kernel instead of the slow density correlators $F_{ij}^{s}(k, t)$ and $\phi(k, t)$, the integral in eqn (1) is reduced to an effective friction term, which encodes the intermolecular static correlations. By solving eqn (1) in this Markovian limit, we find the same qualitative features of Fig. 5. However, this procedure does not provide the correct time scale, which is affected by the structural α-relaxation controlling the decay of $F_{ij}^{s}(k, t)$ and $\phi(k, t)$. MCT provides a microscopic basis for the time scale and the friction (see above), which is a fit parameter in the mentioned phenomenological models. It also provides a unified theoretical approach for chain and glassy dynamics, down to time scales around and before the α-process, which is implicitly 'coarse-grained' within the phenomenological models.
32 G. Allegra and F. Ganazzoli, *Adv. Chem. Phys.*, 1989, **75**, 265–348.
33 L. Harnau, R. G. Winkler and P. Reineker, *J. Chem. Phys.*, 1995, **102**, 7750–7757.